International Journal of Mechanical, Industrial and Aerospace Sciences
ISSN: 2517-9950
Vol:7, No:7, 2013

Numerical Investigation into Mixing Performance of Electrokinetically-Driven Power-Law Fluids in Microchannel with Patterned Trapezoid Blocks

Cha'o-Kuang Chen and Ching-Chang Cho

Abstract**—**The study investigates the mixing performance of electrokinetically-driven power-law fluids in a microchannel containing patterned trapezoid blocks. The effects of the geometry parameters of the patterned trapezoid blocks and the flow behavior index in the power-law model on the mixing efficiency within the microchannel are explored. The results show that the mixing efficiency can be improved by increasing the width of the blocks and extending the length of upper surface of the blocks. In addition, the results show that the mixing efficiency increases with an increasing flow behavior index. Furthermore, it is shown that a heterogeneous patterning of the zeta potential on the upper surfaces of the trapezoid blocks prompts the formation of local flow recirculations, and therefore improves the mixing efficiency. Consequently, it is shown that the mixing performance improves with an increasing magnitude of the heterogeneous surface zeta potential.

Keywords**—**Non-Newtonian fluid, Power-law fluid, Electroosmotic flow, Passive mixer, Mixing, Micromixer.

I. Introduction

SAMPLE mixing is a critical process in many microfluidic applications, including biological and chemical analyses, drug delivery, DNA hybridization, and so forth. However, obtaining an efficient mixing effect in microfluidic systems is difficult since the small characteristic scale of microfluidic devices constrains the fluid flow to the low Reynolds number regime, and thus species mixing occurs primarily as a result of diffusion (an inherently slow process). As a result, a requirement exists for efficient micromixing schemes.

Existing micromixing strategies can be broadly classified as either active or passive. In active mixing schemes, the samples are mixed via the application of external time-varying perturbation forces, e.g., pressure perturbations [1], [2], electrical perturbations [3], [4], and so forth. By contrast, in passive mixing schemes, the samples are mixed via the flow disturbances induced within microchannels with specifically-designed geometries, e.g., staggered herringbone microchannels [5], [6], three-dimensional serpentine microchannels [7], [8], wave form microchannels [9], [10], and so on. Of the two types of mixing scheme, passive schemes are widely preferred since they are more easily integrated with other microfluidic devices, require no additional perturbation source, and have a greater reliability due to the absence of moving parts.

The studies mentioned above all consider the flow of a Newtonian fluid. However, in many practical microfluidic applications (e.g., those involving bio-fluids), the fluid is actually non-Newtonian. As a result, the rheological behavior of the fluid must be taken into account. In addition, fluid transport in microfluidic systems is most commonly achieved via electroosmotic flow (EOF) due to its plug-like velocity profile, lack of moving parts, and high repeatability and reliability. Consequently, the problem of non-Newtonian EOF has attracted increasing attention in recent years [11]-[15]. Overall, the results presented in [11]-[15] showed that the value of the flow behavior index in the power-law model has a significant effect on the flow characteristics. Specifically, for a given set of operating conditions, pseudoplastic fluids (i.e., fluids with a flow behavior index of less than unity) have a higher average velocity than dilatant fluids (i.e., fluids with a flow behavior index greater than unity).

As described above, the literature contains many investigations into the micromixing characteristics of Newtonian fluids. By contrast, the micromixing performance of electrokinetically-driven non-Newtonian fluids has attracted relatively little attention. However, the micromixing behavior of such fluids is of significant interest since many of the fluids used in practical microfluidic systems are non-Newtonian. Accordingly, this study performs a numerical investigation into the mixing performance of electrokinetically-driven non-Newtonian power-law fluids in microchannels containing patterned trapezoid blocks. The effects on the mixing performance of the block width and flow behavior index in the power-law model are examined. In addition, the mixing improvement obtained by applying heterogeneous surface charge patches to the upper surfaces of the trapezoid blocks is then investigated.

II. Mathematical Formulation

A. Governing Equations and Boundary Conditions

In deriving the governing equations for the non-Newtonian power-law electrokinetically-driven flow within the channel shown in Fig. 1, the following assumptions are made: (i) the samples are both incompressible fluids and have the same

C. K. Chen is with the Department of Mechanical Engineering, National Cheng Kung University, Tainan 70101, Taiwan, ROC (phone: +886-6-2757575-62140; fax: +886-6-2342081; e-mail: ckchen@mail.ncku.edu.tw).

C. C. Cho is with the Department of Mechanical Engineering, National Cheng Kung University, Tainan 70101, Taiwan, ROC (e-mail: cccho@mail.ncku.edu.tw).

diffusion coefficient; (ii) the flow field is two-dimensional and in a steady state; (iii) no chemical reactions take place; (iv) and the gravitational, buoyancy and Joule heating effects are sufficiently small to be ignored. The governing equations of interest include the Poisson-Boltzmann equation, the Laplace equation, the continuity equation, the modified Cauchy momentum equation and the convection-diffusion equation. For symmetric electrolytes, these governing equations can be written respectively as follows [15]:

$$\nabla^2\psi = \frac{2n_0 ze}{\varepsilon\varepsilon_0}\sinh\left(\frac{ze}{k_B T_a}\psi\right) \tag{1}$$

$$\nabla^2\phi = 0 \tag{2}$$

$$\nabla\cdot\vec{V} = 0 \tag{3}$$

$$\begin{aligned}\rho(\vec{V}\cdot\nabla)\vec{V} &= -\nabla P \\ &+ \nabla\cdot\eta[\nabla\vec{V} + (\nabla\vec{V})^T] \\ &+ 2n_0 ze[\sinh(\frac{ze}{k_b T}\psi)][\nabla(\psi+\phi)]\end{aligned} \tag{4}$$

$$(\vec{V}\cdot\nabla)C = D\nabla^2 C \tag{5}$$

where ψ is the potential induced by the charge on the walls; n_0 is the bulk concentration of the ions; z is the ionic valence; e is the elementary charge; ε is the dielectric constant of the electrolyte solution; ε_0 is the permittivity of a vacuum; k_B is the Boltzmann constant; T_a is the absolute temperature; ϕ is the applied electric potential; ρ is the fluid density; $\vec{V}$ is the velocity vector with components u and v in the x- and y-directions, respectively; P is the pressure; η is the shear viscosity; C is the sample concentration; D is the diffusion coefficient; and T denotes transposition. Note that the last term in (4) represents the electrokinetic driving body force.

For a non-Newtonian fluid, the dynamic viscosity can be described by the following power-law model [15]:

$$\mu = m\dot{\gamma}^{n-1} \tag{6}$$

where m is the flow consistency index, n is the flow behavior index, and $\dot{\gamma}$ is the shear rate. If the flow behavior index has a value of $n<1$, the fluid is said to be pseudoplastic. Conversely, if the flow behavior index has a value of $n>1$, the fluid is said to be dilatant. Finally, if the flow behavior index has a value of $n=1$, the fluid is Newtonian.

In simulating the flow within the microchannels shown in Fig. 1, it is assumed that the two non-Newtonian power-law fluids are injected electrokinetically into the microchannel via two separate inlets. A constant electric potential is applied at the two inlets and a reference electric potential is set at the outlet. Meanwhile, a no-slip velocity boundary condition is imposed on all the wall surfaces. The boundary conditions at the inlets, outlet and wall surface are therefore specified as

Inlets:

$$\nabla\psi\cdot\vec{n}_\perp = 0,\ \phi = \phi_{in};\ p = 0;\ C = C_A \text{ or } C_B$$

Outlet:

$$\nabla\psi\cdot\vec{n}_\perp = 0,\ \phi = \phi_{out};\ p = 0;\ \nabla C\cdot\vec{n}_\perp = 0$$

Wall surface:

$$\psi = \zeta_w,\ \nabla\phi\cdot\vec{n}_\perp = 0,\ \vec{V} = 0;\ \nabla C\cdot\vec{n}_\perp = 0$$

where ϕ_{in} and ϕ_{out} are the externally applied electric potentials at the inlets and outlet, respectively; C_A and C_B are the concentrations of samples A and B, respectively; ζ_w is the zeta potential on the wall surface; and $\vec{n}_\perp$ denotes the normal vector.

B. Numerical Solution Procedure

The geometry configuration shown in Fig. 1 is a non-orthogonal system. Therefore, in analyzing the flow in the microchannel, the governing equations given in (1) ~ (5) must be transformed from a Cartesian coordinate system to a generalized curvilinear coordinate system. The transformed governing equations have the following generalized form [15]:

$$\begin{aligned}\frac{\partial}{\partial\xi}(\rho_\phi U f) + \frac{\partial}{\partial\eta}(\rho_\phi V f) &= \frac{\partial}{\partial\xi}[\frac{\Gamma_\phi}{J}(\alpha_\phi\frac{\partial f}{\partial\xi} - \beta_\phi\frac{\partial f}{\partial\eta})] \\ &+ \frac{\partial}{\partial\eta}[\frac{\Gamma_\phi}{J}(-\beta_\phi\frac{\partial f}{\partial\xi} + \gamma_\phi\frac{\partial f}{\partial\eta})] \\ &+ JS_\phi\end{aligned} \tag{7}$$

where f is a generalized variable; ξ and η are the two axes of the transformed coordinate system; U_t and V_t are the velocity components in the transformed coordinate system; S_t is a source term; α_t, β_t and γ_t are parameters of the transformed coordinates, respectively; and J is the Jacobian factor. Note that a body-fitted grid system used to model the geometry configuration is generated by solving a set of Poisson equations [16].

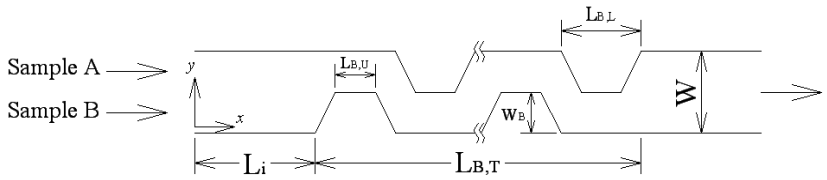

Fig. 1 Schematic illustration of microchannels containing patterned trapezoid blocks

In performing the simulations, the governing equations and boundary conditions were solved using the finite-volume numerical method [17]. A second-order scheme was used to discretize the convection terms and the velocity and pressure fields were coupled using the SIMPLE algorithm [17]. Finally, the discretized algebraic equations were solved using the TDMA (tri-diagonal matrix algorithm) scheme.

C. Mixing Efficiency

The mixing performance within the microchannel was quantified by evaluating the mixing efficiency (η_m) at various cross-sections of the microchannel in accordance with [10]

$$\eta_m = \left[1 - \frac{\int_{-L_c/2}^{L_c/2} |C - C_\infty| d\eta}{\int_{-L_c/2}^{L_c/2} |C_0 - C_\infty| d\eta} \right] \times 100\% \qquad (8)$$

where C is the sample concentration, and C_0 and C_∞ are the sample concentrations in the completely unmixed and completely mixed conditions, respectively. Thus, a mixing efficiency of $\eta_m = 100\%$ indicates a perfectly mixed state, while a mixing efficiency of $\eta_m = 0\%$ indicates a completely unmixed state

D. Numerical Validation

To validate the numerical model described above, the numerical results for the u-velocity distributions of a power-law fluid ($n = 0.5$) and a Newtonian fluid ($n = 1.0$) within a parallel-plate channel were compared with the corresponding analytical solutions. Under the assumption of the Debye-Huckel linearization, the analytical solutions for the two *u*-velocity distributions are given as follows [11]:

$$n = 0.5: \quad u = \frac{\mathrm{K}}{2}\left(-\frac{\varepsilon\varepsilon_0\zeta_w E}{m}\right)^2 \times \frac{\sinh(2\mathrm{K}W - \sinh(2\mathrm{K}y) - 2(\mathrm{K}W - \mathrm{K}y))}{2\cosh^2(\mathrm{K}W)} \qquad (9)$$

$$n = 1.0: \quad u = -\frac{\varepsilon\varepsilon_0\zeta_w E}{m}\left[1 - \frac{\cosh(\mathrm{K}y)}{\cosh(\mathrm{K}W)}\right] \qquad (10)$$

Note that E is the intensity of the applied electric field, $\mathrm{K} = \left(\frac{2n_0 z^2 e^2}{\varepsilon\varepsilon_0 k_B T_a}\right)^{1/2}$ is the Debye-Hückel parameter and K^{-1} is the characteristic thickness of the EDL. Note also that the non-dimensional Debye-Hückel parameter (κ) is defined as $\kappa = \mathrm{K} \times W$. Fig. 2 compares the numerical and analytical results for the non-dimensional u-velocity distributions of the two fluids. (Note that the microchannel is assumed to be symmetric about the horizontal centerline and to have a half-width of *W*.) It is seen that a good agreement exists between the numerical and analytical results for both fluids. In other words, the basic validity of the numerical model is confirmed.

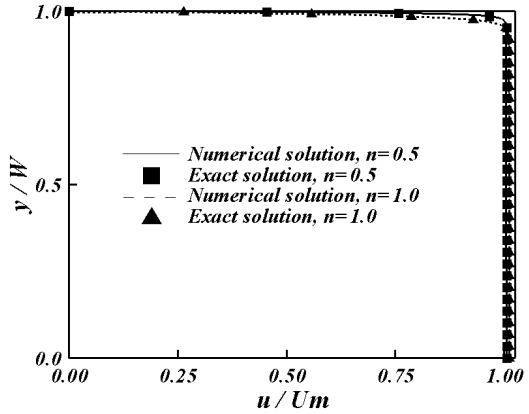

Fig. 2 Comparison of exact and numerical solutions for non-dimensional *u*-velocity distributions of pseudoplastic and Newtonian fluids in parallel-plate microchannel. Note that the non-dimensional Debye-Hückel parameter is specified as $\kappa = 100$. Note also that U_m indicates the mean velocity in the microchannel

III. Results and Discussion

In performing the simulations, it was assumed that the electric field strength was set as E=200 V/cm, the zeta potential was taken as $\zeta_w = -50mV$, the flow consistency index in the power-law model was given as $m = 1\times10^{-3} Pa\cdot s^n$, and the diffusion coefficient of the two samples was set as $D = 1\times10^{-10} m^2 s^{-1}$. In addition, the length of the lower surface of the trapezoid blocks is given as $L_{B,L} = 1W$ and the total length of the block region is assigned as $L_{B,T} = 10W$. The other physical properties of the fluid were specified as follows: fluid density, $\rho = 10^3 kgm^{-3}$; Boltzmann constant, $k_B = 1.3081\times10^{-23} JK^{-1}$; absolute temperature, $T_a = 300K$; permittivity of vacuum, $\varepsilon_0 = 8.854\times10^{-12} Fm^{-1}$; dielectric constant of medium, $\varepsilon = 80$; elementary charge,

$e = 1.6021 \times 10^{-19} C$; ionic valency, $z = 1$; and the non-dimensional Debye-Huckel parameter, $\kappa = 100$.

Figs. 3 (a) and (b) illustrate the flow streamlines and sample concentration in the microchannel containing patterned trapezoid blocks, respectively. Note that a homogeneous zeta potential is used on all wall surfaces. In EOF, an electrokinetic driving force is induced by the interaction between the EDL potential and the externally-applied electric field. Since the electrokinetic driving force acts only on the fluid near the wall surface and to drag the bulk fluid within the microchannel, it can be seen that the flow streamlines follow the surface and no flow separation occurs (see Fig. 3 (a)). As the samples flow over the block surfaces in the microchannel, the interfacial contact area between them is increased. Consequently, the mixing performance is improved (see Fig. 3 (b)).

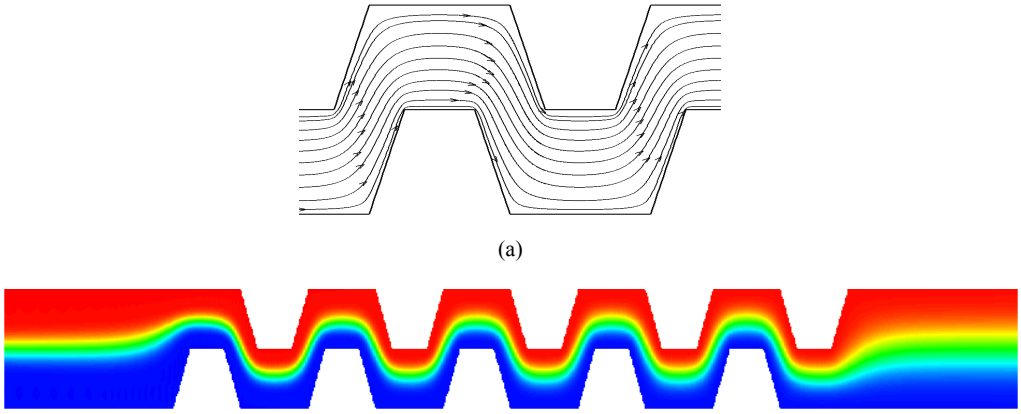

(a)

(b)

Fig. 3 (a) Flow streamlines, and (b) sample concentration distribution in microchannel with homogeneous surface charge pattern. Note that $n = 0.8$, $W_B = 0.5W$ and $L_{B,U} = 0.5W$

Fig. 4 shows the variation of the mixing efficiency at $x = 30W$ with the flow behavior index as a function of the block width (W_B). In microchannels, sample mixing takes place primarily as a result of diffusion. As discussed above, in the microchannels considered in this study, the blocks increase the interfacial contact area between the two samples. Moreover, the increase in the interfacial contact area increases with an increasing block width. Thus, as shown in Fig. 4, the mixing efficiency increases as the block width is increased. For power-law fluids, the viscosity reduces with a reducing value of the flow behavior index. Consequently, the volumetric flow rate increases as the flow behavior index decreases. In addition, the fluid flow in microchannles is confined to the low Reynolds number regime. Therefore, when the fluid passes through a microchannel with patterned trapezoid blocks, flow recirculations are not easily formed. In other words, as the volumetric flow rate increases, the fluid passes more rapidly through the microchannel, but the perturbation of the fluid is not significantly increased. Therefore, not only is the mixing time reduced, but there is no significant increase in the interfacial contact area between the two species. As a result, the mixing efficiency reduces as the flow behavior index reduces.

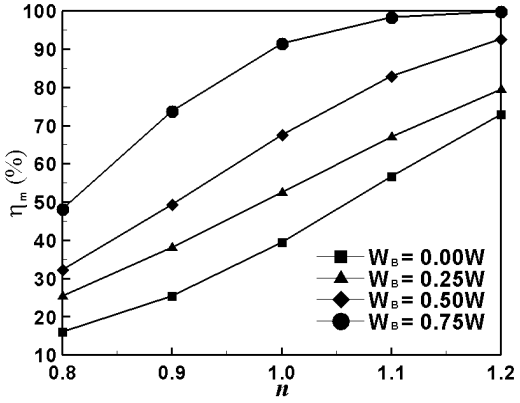

Fig. 4 Variation of mixing efficiency at $x = 30W$ with flow behavior index n as function of block width W_B. Note that $L_{B,U} = 0.5W$

Fig. 5 shows the variation of the mixing efficiency at $x = 30W$ with the flow behavior index as a function of the length of the upper surface of the trapezoid blocks ($L_{B,U}$). It can be expected that extending the length of $L_{B,U}$ increases the interfacial contact area between the samples, and thus the diffusion effect is enhanced. Therefore, as shown in Fig. 5, the mixing efficiency improves as $L_{B,U}$ is increased.

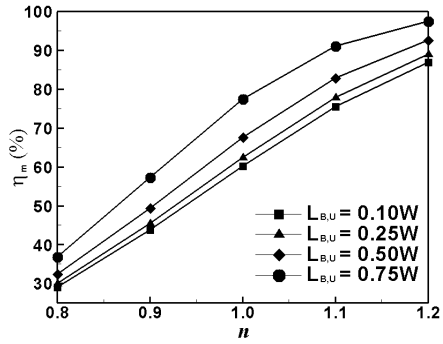

Fig. 5 Variation of mixing efficiency at $x = 30W$ with flow behavior index n as function of length of upper surface of block $L_{B,U}$. Note that $W_B = 0.5W$

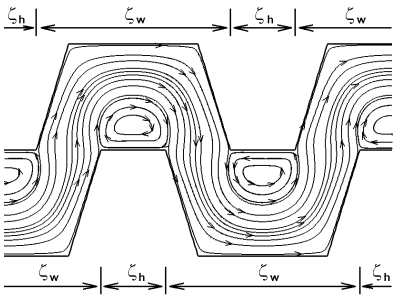

(a)

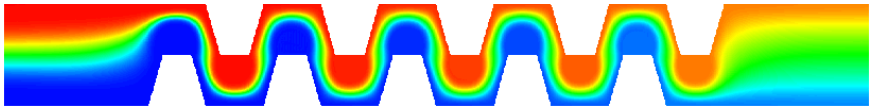

(b)

Fig. 6 (a) Flow streamlines, and (b) sample concentration distribution in microchannel with heterogeneous surface charge pattern. Note that $n = 0.8$, $W_B = 0.5W$ and $L_{B,U} = 0.5W$

Figs. 6 (a) and (b) illustrate the flow streamlines and sample concentration in a microchannel with heterogeneous surface charge patches on the upper surfaces of the trapezoid blocks. Note that the zeta potential on the heterogeneous surfaces is set as ζ_h and has a value of $\zeta_h = -|\zeta_w|$. When heterogeneous patches are applied on the local surface of a microchannel, the heterogeneous surface regions absorb the opposite electric charge to the original regions of the surface. The regions of opposite surface charge affect the EDL potential distribution within the microchannel. Thus, when an external electric field is applied to the microchannel, the flow in the region of the heterogeneous patches moves in the opposite direction to that in the region of the original surface. The interaction between the local flow and the bulk flow induces flow recirculations near the heterogeneous surfaces (see Fig. 6 (a)).

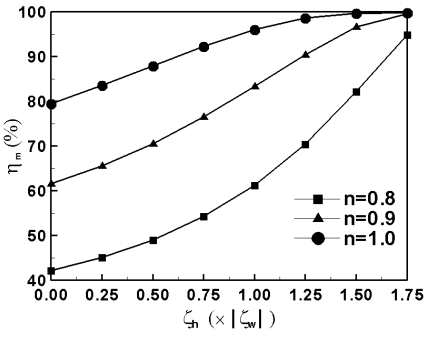

Fig. 7 Variation of mixing efficiency at $x = 30W$ with magnitude of heterogeneous surface zeta potential ζ_h as function of flow behavior index n. Note that $W_B = 0.5W$ and $L_{B,U} = 0.5W$

The flow recirculations perturb the flow field and therefore increase the interfacial contact area between the samples (see Fig. 6 (b)). As a result, the mixing efficiency is improved.

Fig. 7 shows the variation of the mixing efficiency with the magnitude of the heterogeneous surface zeta potential as a function of the flow behavior index. Note that in the figure, pseudoplastic fluids and Newtonian fluids are only discussed since, for dilatant fluids, a high mixing performance is obtained by patterning the blocks in the microchannel (see Figs. 4 and 5). It is shown that the mixing performance improves with an increasing magnitude of the heterogeneous surface zeta potential. As the magnitude of the zeta potential increases, the size of the flow recirculation structures near the heterogeneous surface regions also increases. As a result, the interfacial contact area between the samples increases and the mixing performance is improved. In other words, patterning the heterogeneous surface charge patch on the microchannel surfaces is beneficial in enhancing the mixing performance.

IV. Conclusions

This study has investigated the mixing characteristics of electrokinetically-driven power-law fluids in a microchannel containing patterned trapezoid blocks. The effects on the mixing performance of the geometry parameters and the flow behavior index in the power-law model have been examined. The results have shown that the mixing performance can be improved by increasing the width of the blocks or increasing the length of upper surface of the blocks. The results have also shown that dilatant fluids have a better mixing efficiency than pseudoplastic fluids. In addition, it has been shown that a heterogeneous patterning of the zeta potential on the upper

surfaces of the blocks prompts the formation of flow recirculations in the microchannel, and therefore improves the mixing performance. Consequently, an effective enhancement in the mixing efficiency can be obtained by increasing the magnitude of the heterogeneous surface zeta potential.

ACKNOWLEDGMENT

The authors would like to thank the National Science Council of the Republic of China, Taiwan, for financially supporting this research under Contract No. 101-2221-E-006-092-MY2.

REFERENCES

[1] X. Niu, and Y. K. Lee, "Efficient spatial-temporal chaotic mixing in microchannels," J. Micromech. Microeng., Vol. 13, no. 3, pp. 454-462, May 2003.
[2] C. C. Cho, C. L. Chen, R. T. Tsai, and C.K. Chen, "A novel microfluidic mixer using aperiodic perturbation flows," Chem. Eng. Sci., Vol. 66, no. 23, pp. 6159-6167, Dec.2011..
[3] J. R. Pacheco, K. P. Chen, A. Pacheco-Vega, B. Chen, and M. A. Hayes, "Chaotic mixing enhancement in electro-osmotic flows by random period modulation," Phys. Lett. A, Vol. 372, no. 7, pp. 1001-1008, Feb. 2008.
[4] C. C. Cho, C. L. Chen, and C. K. Chen, "Mixing enhancement in crisscross micromixer using aperiodic electrokinetic perturbing flows," *Int. J. Heat Mass Transf.*, Vol. 55, no. 11-12, pp. 2926-2933, May 2012.
[5] A. D. Stroock, S. K. W. Dertinger, A. Ajdari, I. Mezic, H. A. Stone, and G. M. Whitesides, "Chaotic mixer for microchannels," Science, Vol. 295, no. 555, pp. 647-651, Jan. 2002.
[6] R. Choudhary, T. Bhakat, R. K. Singh, A. Ghubade, S. Mandal, A. Ghosh, A. Rammohan, A. Sharma, and S. Bhattacharya, "Bilayer staggered herringbone micro-mixers with symmetric and asymmetric geometries," Microfluid. Nanofluid., Vol. 10, no. 2, pp. 271-286, Feb. 2011.
[7] R. H. Liu, M. A. Stremler, K. V. Sharp, M. G. Olsen, J. G. Santiago, R. J. Adrian, H. Aref, and D. J. Beeber, "Passive mixing in a three-dimensional serpentine microchannel," J. Microelectromech. Syst., Vol. 9, no. 2, pp. 190-197, Jun. 2000.
[8] M. A. Ansari, and K. Y. Kim, "Parametric study on mixing of two fluids in a three-dimensional serpentine microchannel," Chem. Eng. J., Vol. 146, no. 3, pp. 439-448, Feb. 2009.
[9] V. Mengeaud, J. Josserand, and H. H. Girault, "Mixing processes in a zigzag microchannel: finite element simulations and optical study," Anal. Chem., Vol. 74, no. 16, pp. 4279-4286, Aug. 2002.
[10] C. K. Chen, and C.C. Cho, "Electrokinetically-driven flow mixing in microchannels with wavy surface," J. *Colloid Interface Sci.*, Vol. 312, no. 2, pp. 470-480, Aug. 2007.
[11] C. Zhao, E. Zholkovskij, J. H. Masliyah, and C. Yang, "Analysis of electroosmotic flow of power-law fluids in a slit microchannel," J. Colloid Interface Sci., Vol. 326, no. 2, pp. 503-510, Oct. 2008.
[12] G. H. Tang, X. F. Li, Y. L. He, and W. Q. Tao, "Electroosmotic flow of non-Newtonian fluid in microchannels," J. Non-Newton. Fluid Mech., Vol. 157, no. 1-2, pp. 133-137, Mar. 2009.
[13] N. Vasu, and S. De, "Electroosmotic flow of power-law fluids at high zeta potentials," Colloid Surf. A-Physicochem. Eng. Asp., Vol. 368, no. 1-3, pp. 44-52, Sep. 2010.
[14] M. Hadigol, R. Nosrati, and M. Raisee, "Numerical analysis of mixed electroosmotic/pressure driven flow of power-law fluids in microchannels and micropumps," Colloid Surf. A-Physicochem. Eng. Asp.. Vol. 374, no. 1-3, pp. 142-153, Jan. 2011.
[15] C. C. Cho, C. L. Chen, and C. K. Chen, "Electrokinetically-driven non-Newtonian fluid flow in rough microchannel with complex-wavy surface," J. Non-Newton. Fluid Mech., Vol. 173-174, pp. 13-20, Apr. 2012.
[16] P. D. Thomas, and J. F. Middlecoff, "Direct control of the grid point distribution in meshes generated by elliptic equations," *AIAA J.*, Vol. 18, no. 6, pp. 652-656, 1980.
[17] S. V. Patankar, "Numerical Heat Transfer and Fluid Flow," New York: McGraw-Hill, 1980.

Prof. Cha'o-Kuang Chen is currently National Chair Professor of Mechanical Engineering Department at National Cheng Kung University, Tainan, Taiwan, ROC. He received his B.S. degree in mechanical engineering from National Cheng Kung University, Tainan, Taiwan, in 1958, his Master of Mechanical Engineering from Georgia Institute of Technology, Atlanta, Ga., in 1970, and his Ph.D. in mechanical engineering from the University of Liverpool, UK, in 1986. He was the head of the Department of Mechanical Engineering in 1990–1993. His current research interests include nonlinear stability analysis of Newtonian and non-Newtonian fluid flows, thermal stability analysis of electro-magneto-fluids, finite-time thermodynamic cycles and thermal efficiency analysis, fuzzy control and optimal design, molecular dynamics simulation, nanotechnology, heat/mass transfer in micro/nano-scales, thermal economics, and Lattice Boltzmann method.

Dr. Ching-Chang Cho is currently a postdoctoral fellow at the Department of Mechanical Engineering, National Cheng Kung University, Taiwan. He received his Ph.D. in mechanical engineering from National Cheng Kung University, Taiwan, in 2009. His major research areas include electroosmotic flow, micromixer, and heat/mass transfer enhancement. He has published over 20 SCI/EI papers in international journals.